Free Radical Motion in Super Critical Fluids Probed by EPR Spectroscopy

S. N. Batchelor[†]

Physikalisch-Chemisches Institut der Universität Zürich, Winterthurerstrasse 190, CH-8057 Zürich, Switzerland

Received: July 17, 1997; In Final Form: November 10, 1997

EPR spectra of the nitroxide radical 2,2,6,6-tetramethyl-1-piperidinyloxy (TEMPO) are reported in super critical and in liquid *n*-hexane and ethanol for 25−200 bar and 295−600 K. At low radical concentration ($<10^{-5}$ M) the line width is controlled by the spin-rotation interaction and is quantitatively predicted by liquid-phase theory for solvent densities ρ greater than the critical density ρ_c. Deviations at lower densities are assigned to clustering effects and the crossover to gas-phase behavior. Rate constants for Heisenberg spin exchange ([TEMPO] > 10^{-3} M) up to 580 K are also reported. They again follow liquid-phase theory for $\rho > \rho_c$. Deviations at low densities may be explained by a gas-phase behavior without clustering effects.

Introduction

EPR spectroscopy has been frequently applied to the study of persistent nitroxide radicals in various media.[1] One attractive feature of such studies is that the analysis of the resonance line shapes gives information on the motion and the local environment of the radicals which is difficult to obtain otherwise. Little work[2,3] has been done in this area on super critical fluids (SCFs), which are currently under active investigation as versatile,[4] cheap, and benign media for chemical reactions.[5] Particularly for radical synthesis,[6] it would be useful to know under what conditions the molecular motion is liquid- or gaslike and what effects the local density augmentations near the critical point, that is, critical clustering, may have. Pioneering work has shown that the encounter rate constants of benzyl radicals are liquidlike in SC carbon dioxide, ethane, and trifluoromethane;[7,8] however, in this work the transition region to the gas phase was not reached.[9−11] EPR studies of spin exchange and the hyperfine couplings of di-*tert*-butyl nitroxide in the same solvents over a wide range of pressures at temperatures near T_c showed similar results.[3] Near the critical point these authors found some deviation from liquid behavior and assigned these to critical clustering effects on the radical motion; similar effects where also found in their molecular dynamic simulations.[12,13] For a full picture there is a need for more experimental data on a wider range of SCFs and under a wider range of conditions. EPR investigations of nitroxides appear helpful, and here the 2,2,6,6-tetramethyl-1-piperidinyloxy radical (TEMPO) is studied in SC and liquid ethanol and *n*-hexane in the ranges 295−600 K and 25−200 bar. The solvents chosen have very different properties, for example, molar volumes, T_c, and hydrogen bonding (ethanol),[14,15] from those previously investigated and should help indicate any solvent-specific effects. Information on the radical motion is gained by analysis of the spin rotation and Heisenberg spin-exchange[16] contribution to the EPR line widths. The earlier EPR work[3] did not include an analysis of the spin-rotation contribution and was limited to a much smaller temperature range.

Experimental Section

The apparatus for SCF EPR is an adaptation of one previously described.[17,18,19] In brief, deoxygenated solutions are pressurized and pumped through the TE105 cavity of the EPR spectrometer (Bruker X-Band ESP 300) using a HPLC pump. Stainless steel high-pressure tubing is used except for a quartz capillary section that traverses the cavity. In a change from the original design, the glass-to-metal seals are now achieved using epoxy resin. Room-temperature tests showed that for a capillary of o.d = 4.8 mm, i.d. = 1.4 mm, and 320 mm length the system withstood 400 bar. For safety 250 bar was set as the maximum pressure, and aromatic solvents were avoided because they attack the glue. Care is also taken to keep the upper seal below 320 K by cooling with compressed air. The sample is heated using a commercial device (Wilmad WG-838,836) by flowing hot nitrogen through the EPR dewar surrounding the capillary. Temperatures are measured by a thermocouple between the dewar and the capillary at the top of the cavity, which gives the temperature of the nitrogen. A temperature-dependent correction factor is applied to take account of the drop in temperature between the center and top of the cavity. Relative temperatures are estimated to be accurate to ±5 K and absolute values to ±15 K. Solution flow rates were typically 0.4-1.2 mL min^{-1}, which when combined with the density of the fluids gives residence times of approximately 1−20 s in the hot region.

TEMPO was obtained in its purest available commercial form and the solvents were obtained in HPLC grade; all were used as supplied.

The spin rotation contribution was obtained from the peak-to-peak EPR line width, ΔH_{pp}, of nominally 3×10^{-5} M solutions of TEMPO as functions of temperature and pressure. At this low concentration spin-exchange has no effect. The spin-exchange rate constants were then obtained by recording spectra of nominally 10^{-2} M solutions of TEMPO, again under various conditions, and fitting them with standard literature methods involving the solution of the steady-state Bloch equations.[20] The fit procedure took account of the spin-rotation contribution and the intrinsic line width by inserting appropriate values of T_2. The exact concentration of TEMPO for each condition was obtained by double integration of the spectra and comparison with room-temperature data, allowing for the Boltzmann factor.

[†] Current address: Unilever Research Port Sunlight Laboratory, Quarry Road East, Bebington, Wirral L63 3JW, England. E-mail: Stephen.Batchelor@unilever.com.

S1089-5647(97)02346-8 CCC: $15.00
Published on Web 01/15/1998

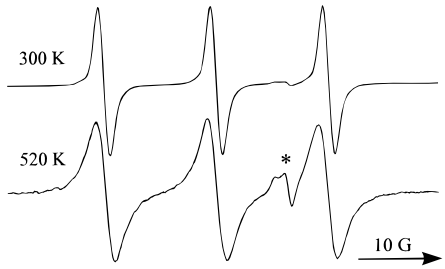

Figure 1. EPR spectra of nominally 3×10^{-5} M TEMPO in *n*-hexane at 27.5 bar. The signal marked with an asterisk arises from the dewar.

TABLE 1: Critical Constants of the Solvents[15]

	ethane	*n*-hexane	ethanol
T_c/K	305	508	514
P_c/bar	48.8	30.1	61.3
ρ_c/mol L^{-1}	6.76	2.70	5.99

Above approximately 550 K TEMPO began to decay on the time scale of the experiment, which was negated by the use of higher flow rates. Lower densities at lower pressures gave the highest flow rates and allowed the highest temperatures. Nevertheless, the decay precluded spin-exchange measurements above 580 K.

Results and Discussion

(i) Spin Rotation. At low concentration the line width is very sensitive to temperature and pressure. Increasing the temperature at constant pressure leads to a large increase, whereas increasing the pressure at constant temperature led to a decrease. The former is illustrated in Figure 1. The critical temperature and pressure, T_c and P_c, of *n*-hexane are 508 K and 30.1 bar, Table 1, and hence the 520 K spectrum is recorded under SC conditions.

The upper part of Figure 2 shows the effect of temperature on ΔH_{pp}, for *n*-hexane and two pressures. At 70 bar ($2.3P_c$) ΔH_{pp} increases gradually with temperature, but at 31 bar ($1.03P_c$) there is a sharp increase above T_c. The pressure dependence at 520 K ($T_c = 508$ K) is shown in the lower part of the figure, and here ΔH_{pp} increases gradually with decreasing pressure until approximately 40 bar ($1.3P_c$), when there is a sharp rise. Ethanol solution gives similar results, as displayed in Figure 3.

For liquids the spin-rotation contribution to the line width is given by[18,21,22]

$$\Delta H_{pp} = 4(3\pi d^3)^{-1}(\Delta g_{||}^2 + 2\Delta g_{\perp}^2)kT/\eta \qquad (1)$$

where d is the radical diameter, $(\Delta g_{||}^2 + 2\Delta g_{\perp}^2)$ is its *g*-anisotropy, and a Gaussian line shape is assumed. For ethanol and *n*-hexane good agreement was found with this equation at high pressures, since ΔH_{pp} shows a linear dependence on T/η, Figure 4, although there are deviations from eq 1 for ethanol above $T/\eta = 15 \times 10^6$ K N^{-1} s^{-1} m^2. The slopes of the lines are identical within experimental error and give $(\Delta g_{||}^2 + 2\Delta g_{\perp}^2) = 7.6 \times 10^{-6}$ when combined with the 0.68-nm diameter of TEMPO as calculated from increments.[23] Although this is an order of magnitude smaller than the value measured directly by EPR[24] of 8.6×10^{-5}, such disagreements are common with this theory,[22] the *g*-anisotropy effectively only acting as a proportionality constant.

Using the *g*-anisotropy from Figure 4 and eq 1, the temperature and pressure dependencies of ΔH_{pp} were calculated and

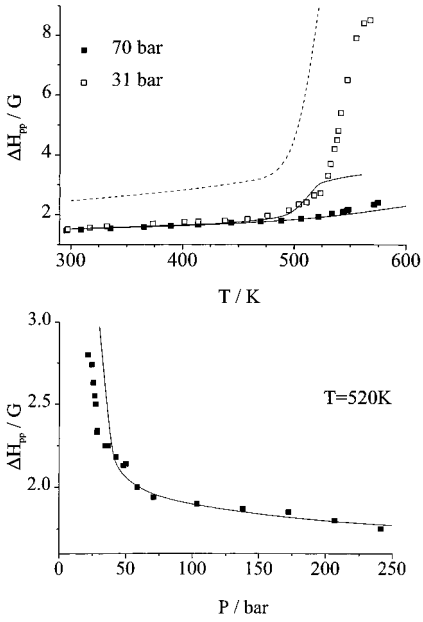

Figure 2. Experimental values of the peak-to-peak linewidth, ΔH_{pp}, of nominally 3×10^{-5} M TEMPO in *n*-hexane as a function of temperature and pressure. The solid lines are the values expected for liquid-phase behavior and the hatched lines for gas-phase behavior.

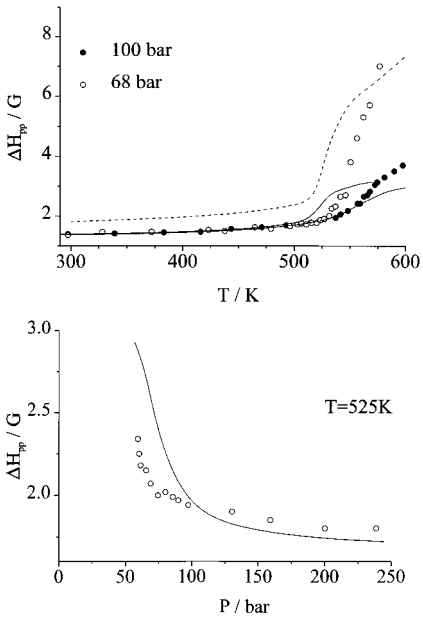

Figure 3. Experimental values of the peak-to-peak line width, ΔH_{pp}, of nominally 3×10^{-5} M TEMPO in ethanol as a function of temperature and pressure. The solid lines are the values expected for liquid-phase behavior, and the hatched lines for gas-phase behavior.

are plotted in Figures 2 and 3 as solid lines. In both solvents the temperature dependencies follow eq 1 at lower pressures until the critical temperatures are reached. Then ΔH_{pp} becomes slightly smaller than expected before it rapidly increases to 8−9 G. A lower than expected ΔH_{pp} is also observed in the pressure dependencies at pressures near P_c.

Equation 1 is valid as far as the Stokes−Einstein equation is obeyed, and the rotational correlation time is much smaller than the reorientation correlation time.[21,22] Calculations of the correlation times using the liquid-phase formula indicate that the second condition is likely to be met under all conditions used here,[18] mainly because of the relatively large size of TEMPO. Consequently, the observed disagreements show

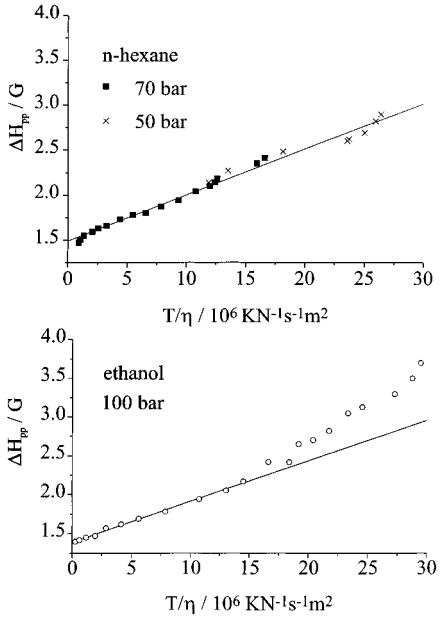

Figure 4. Peak-to-peak line width, ΔH_{pp}, of nominally 3×10^{-5} M TEMPO as a function of T/η for ethanol and *n*-hexane. The lines represent $1.49 + 5.1 \times 10^{-8}$ T/η and $1.39 + 5.2 \times 10^{-8}$ T/η for *n*-hexane and ethanol, respectively.

where the liquid type motion no longer occurs. This is expected to happen when the solution becomes gaslike. In the kinetic gas limit ΔH_{pp} is given by[25]

$$\Delta H_{pp} = \frac{(2\pi\mu kT)^{1/2}}{3I\pi d^2[\text{solvent}]}(\Delta g_{||}^{\ 2} + 2\Delta g_{\perp}^{\ 2}) \qquad (2)$$

where I is the radical moment of inertia and μ is the reduced mass of the solvent and the radical. Equation 2 assumes that each collision changes the rotational state of the radical and, again, a Gaussian line shape. It predicts larger line widths than eq 1. Using the actual solvent concentrations, the values expected in this limit were again calculated and are plotted as hatched lines in Figures 2 and 3. They are not plotted for the pressure dependencies since the values were too large. Obviously, the increases of ΔH_{pp} at high temperatures agree with a transition to the gas-phase behavior. However, the lower values near the critical points do not and are possibly due to critical clustering. Within a cluster the viscosity will not be the same as the bulk viscosity used in eq 1, and furthermore, the motion may not follow Stokes−Einstein, leading to a breakdown of the theory. It is interesting that the clustering effect appears larger in the hydrogen-bonding ethanol.

All deviations from eq 1 appear approximately when the solvent density becomes smaller than the critical density ρ_c, Table 1. This explains why at high pressure *n*-hexane but not ethanol follows eq 1 across the entire T/η range, Figure 4. For *n*-hexane, at the highest temperature the density is 2.8 mol L^{-1}, that is, approximately ρ_c, whereas for ethanol the density drops below ρ_c above $T/\eta = 15 \times 10^6$ K N^{-1} s^{-1} m^2, corresponding to 550 K, 100 bar.

Our finding of liquid behavior for $\rho > \rho_c$ is in agreement with previous results of Troe et al.[10] who found that bromine atom recombinations become diffusion-controlled in SC nitrogen, argon, and neon for $\rho > \rho_c$, although this was not noted explicitly. Molecular dynamics calculations have also shown that the transition from the Stokes−Einstein behavior to the kinetic gas limit starts when ρ approaches ρ_c.[12]

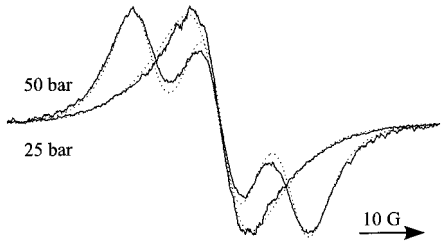

Figure 5. EPR spectra of nominally 10^{-2} M TEMPO in *n*-hexane at 520 K. The dotted lines are fits to the experimental data.

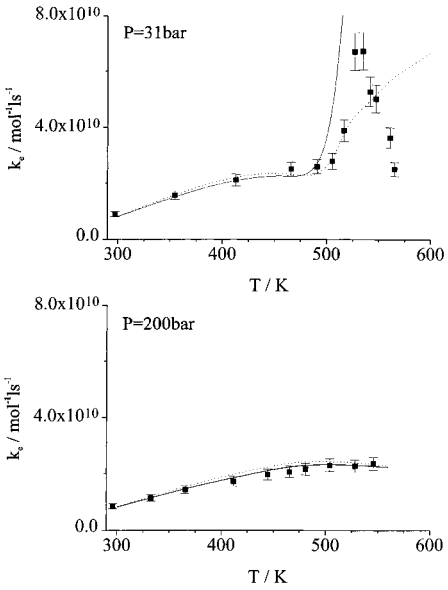

Figure 6. Experimental values of k_e in *n*-hexane as a function of temperature. The dotted and solid lines are simulations using eq 5 and 6, respectively, with parameters given in the text.

(ii) Heisenberg Spin Exchange. At high concentrations of TEMPO the Heisenberg spin exchange strongly affects the line shape of the EPR spectra and was also found to be temperature- and pressure-sensitive. This is illustrated in Figure 5 for nominally 10^{-2} M TEMPO in *n*-hexane, where decreasing the pressure from 50 to 25 bar at 520 K clearly increases the exchange. The rate constant for spin exchange, k_e, was obtained from fits to the spectra, taking into account the actual radical concentration, vide supra.

Figure 6 shows the temperature dependence for *n*-hexane at 200 and 31 bar. At the high pressure there is an increase in k_e with temperature, which levels off at approximately 2.5×10^{10} mol L^{-1} s^{-1}. The behavior is similar at 31 bar until T_c is reached. Then there is a large increase followed by a decrease. A maximum of k_e just above T_c is also observed for ethanol at 68 bar, although the absolute value is smaller, Figure 7. At 100 bar no maximum is observed for ethanol, and k_e gradually rises with temperature. No comparable literature data exiss for SC ethane.[3] The pressure dependencies of k_e at temperatures just above T_c are displayed in Figure 8 and 9 for ethanol, *n*-hexane, and literature data for ethane.[3] All show the same behavior with an increase in k_e as the pressure is lowered toward P_c, although the absolute values are different.

The rate constant for spin exchange, k_e, is given by[16]

$$k_e = k_d \frac{1}{2} \frac{J^2\tau^2}{(1 + J^2\tau^2)} \qquad (3)$$

where τ is the radical−radical encounter time, J is minus two

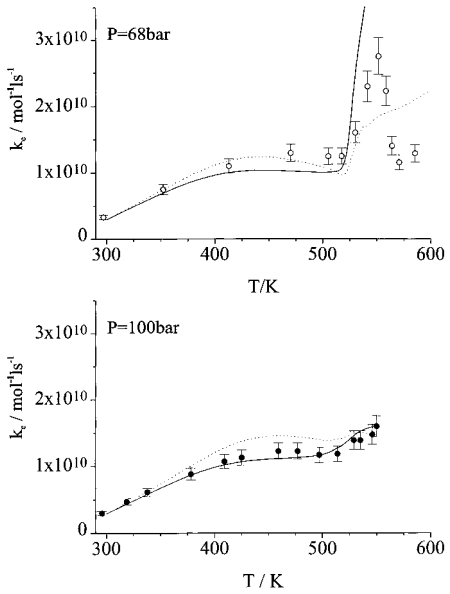

Figure 7. Experimental values of k_e in ethanol as a function of temperature. The dotted and solid lines are simulations using eqs 5 and 6, respectively, with parameters given in the text.

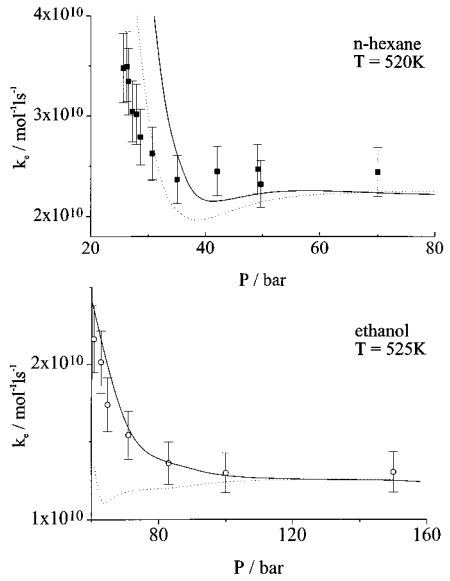

Figure 8. Experimental values of k_e as a function of pressure for *n*-hexane and ethanol. The dotted and solid lines are simulations using eqs 5 and 6, respectively, with parameters given in the text.

times the exchange interaction, and k_d is the encounter rate constant. For the Stokes−Einstein case, k_d is given by

$$k_d = 8RT/3\eta \tag{4}$$

and τ by

$$\tau = \pi d l^2 \eta / 2kT \tag{5}$$

Here, l is the random walk jump length, which has been set equal to $^1/_2 d(\rho(T_m)/\rho(T))^{1/3}$, where T_m is the melting point.[1] The factor involving ρ corrects for density variations[16] and makes τ proportional to $\rho^{-2/3}$; it is however only semiempirical. For nitroxide radicals in the liquid phase normally eq 3-5 describe the spin exchange very well, but Randolph and Carlier[3] showed that near the critical point it underpredicts k_e for SC ethane. This may be due to critical clustering enhancing spin exchange

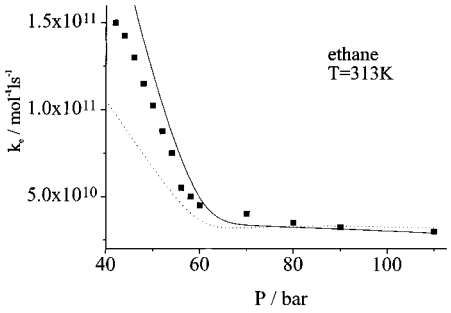

Figure 9. Literature values[3] of k_e for di-*tert*-butyl nitroxide in ethane as a function of pressure. The dotted and solid lines are simulations using eqs 5 and 6, respectively, with parameter values given in the text.

TABLE 2: Values of the Exchange Interaction, *J*, Used To Fit the Experimental Data

	$J/10^{11}$ s^{-1} eq 5	$J/10^{11}$ s^{-1} eq 6
n-hexane	4.1	5.4
ethanol	2.5	6.2
ethane	5.5	5.0

as they suggested[3,12,13] or, more simply, that the density correction used is not valid.

An alternative, novel approach to include effects of solvent density change is to assume that encounter pairs survive until they collide with a solvent molecule. τ is then given by

$$\tau = (k_d[\text{solvent}])^{-1} \tag{6}$$

Effectively this implies a small attractive potential between the TEMPO radicals, which weakly binds the encounter pair together, and may allow crudely for radical−radical clustering. Molecular dynamics calculations on Lennard-Jones molecules with parameters chosen to simulate nitroxide radicals have shown that radical−radical clusters should in fact occur.[13] In comparison to eq 5 the Ansatz 6 increases the density dependence since τ becomes proportional to ρ^{-1}.

Simulations of the experimental data were attempted using both eq 5, and eq 6 for τ. J was assumed to be independent of temperature and pressure but solvent-dependent, and the values chosen are given in Table 2. They are close to the literature value[16] of $J \approx 5 \times 10^{11}$ s^{-1}. For $T > T_c$ solvent concentrations were obtained from the principle of corresponding states combined with graphical data[26] and for $T < T_c$ from extrapolated literature data.[27] To obtain a reasonable simulation of the data of Randolph and Carlier[3] in ethane from eq 6 and a J value close to 5×10^{11} Hz, τ was increased by a factor of 3.3. This seemed reasonable for this model, since the data for ethane were obtained at the rather low temperature of 313 K, where the lower kinetic energy of the molecules renders not all collisions successful in destroying the encounter pairs.

In Figures 6−9 the simulations with eq 5 are displayed with dotted lines, and those with eq 6 with solid lines. For all systems the temperature and the pressure dependencies are described rather reasonably for temperatures lower than T_c and pressures higher than P_c with both equations. The temperature dependence is characterized by an initial increase with T which corresponds to the region where $J\tau > 1$ so that every radical−radical encounter leads to spin exchange and k_e is proportional to T/η. At higher temperatures $J\tau \approx 1$ is reached, where not every encounter is successful. This produces the observed plateau. For still higher temperatures, $J\tau < 1$, so that $k_e = 0.5k_dJ^2\tau^2$ should become proportional to η/T. There a decrease

of k_e would occur; however, the large decrease of the density increases τ and hence k_e. In the pressure dependencies near T_c, Figure 8, the variations in viscosity and density nearly cancel, making k_e virtually pressure-independent above P_c. For lower pressures k_e increases because of the large decrease of ρ.

A breakdown of the models is seen above T_c at low pressures in Figures 6 and 7 and at low pressures in Figure 8 and 9. Under these conditions eq 5, used by Randolph and Carlier,[3] generally underpredicts k_e, eq 6 generally overpredicts, and the experimental data often lie between them. Positive deviation suggests critical clustering,[3] while negative deviation may be attributable to an onset of gas-phase behavior. Previous experimental work[25] roughly estimated that for spin exchange of nitroxide radicals in the gas phase at 300 K only 1 of 25 collisions is effective. With this value, the kinetic gas theory for k_d,

$$k_d = \pi d^2 \left(\frac{4kT}{\pi m}\right)^{1/2} \tag{7}$$

yields $k_e = k_d/25 = 7 \times 10^9$ mol L^{-1} s^{-1} at 550 K, which is lower than k_e calculated for the liquid state and is in reasonable agreement with the experimental 1.2 and 2×10^{10} mol L^{-1} s^{-1} measured for ethanol and *n*-hexane, respectively, at the highest temperatures and lowest pressures. Thus using eq 6, the low-density behavior of k_e may be simply ascribed to the crossover to gas-phase motion without clustering.

Conclusion

Extending previous EPR work on nitroxides in SCFs, it has been found that Heisenberg spin-exchange rate constants do not clearly show effects of critical clustering, when solvent density effects are fully considered, although these may be observed in the spin-rotational contribution to the line width. The liquid-phase formula for radical motion may be applied to SCFs provided the density is less than the critical density.

Acknowledgment. The author thanks Prof. H. Fischer (Zurich) and Dr. A. I. Shushin (Moscow) for useful discussions. Mr. V. V. Tarasov (Zurich) is thanked for the Heisenberg spin-exchange program.

References and Notes

(1) Molin, Yu. N.; Salikhov, K. M.; Zamaraev, K. I. *Spin Exchange: Principles and Applications in Chemistry and Biology*; Springer-Verlag: Berlin, 1980.
(2) Shaulov, A. Yu.; Andreyeva, N. I.; Sklarova, A. G.; Buchachenko, A. L.; Yenikolopyan N. S.; Shaulov, Yu. Kh. *Zh. Eksp. Teor. Khim.* **1972**, *63*, 157.
(3) Randolph, T. W.; Carlier C. *J. Phys. Chem.* **1992**, *96*, 5146. Ganapathy, S.; Carlier, C.; Randolph, T. W.; O'Brien, J. A. *Ind. Eng.Chem. Res.* **1996**, *35*, 19.
(4) Stanley H. E. *Introduction to Phase Transitions and Critical Phenomena*; Oxford University Press: New York, 1971, 1987.
(5) Eckert, C. A.; Knutson, B. L.; Debenedetti, P. G. *Nature* **1996**, *383*, 313.
(6) DeSimone, J. M.; Maury, E. E.; Menceloglu, Y. Z.; McClain, J. B.; Romack, T. J.; Combes, J. R. *Science* **1994**, *265*, 356.
(7) Roberts, C. B.; Zhang, J.; Brennecke, J. F.; Chateauneuf, J. E. *J. Phys. Chem.* **1993**, *97*, 5618.
(8) Roberts, C. B.; Zhang, J.; Chateauneuf, J. E.; Brennecke, J. F. *J. Am. Chem. Soc.* **1993**, *115*, 9576.
(9) Hirschfelder, J. O.; Curtiss, C. F.; Bird, R. B. *Molecular Theory of Gases and Liquids*; John Wiley: New York, 1954.
(10) Hippler, H.; Schubert, V.; Troe, J. *J. Chem. Phys.* **1984**, *81*, 3931.
(11) Hippler, H.; Schubert, V.; Troe, J. *Ber. Bunsen-Ges. Phys. Chem.* **1985**, *89*, 760.
(12) Randolph, T. W.; O'Brien, J. A.; Ganapathy, S. *J. Phys. Chem.* **1994**, *98*, 4173.
(13) Ganapathy, S.; Brien, J. A.; Randolph, T. W. *AIChEJ* **1995**, *41*, 346. Ganapathy, S.; Randolph, T. W.; Carlier, C.; O'Brien, J. A. *Int. J. Thermophys.* **1996**, *17*, 471.
(14) Stephan, K.; Lucas, K. *Viscosity of Dense Fluids*; Plenum Press: New York, 1979.
(15) Lide, D. R., Ed. *Handbook of Chemistry and Physics*; CRC Press, Boca Raton, 1996.
(16) Plachy, W.; Kivelson, D. *J. Chem. Phys.* **1967**, *47*, 3312.
(17) Livingston, R.; Zeldes, H.; Conradi, M. S. *J. Am. Chem. Soc.* **1979**, *101*, 4312.
(18) Batchelor, S. N.; Henningsen, B.; Fischer, H. *J. Phys. Chem. A* **1997**, *101*, 2969.
(19) Livingston, R.; Zeldes, H. *Rev. Sci. Instrum.* **1981**, *52*, 1352.
(20) Johnston, C. S., Jr. *Mol. Phys.* **1967**, *12*, 25.
(21) Hubbard, P. S. *Phys. Rev.* **1963**, *131* 1155.
(22) Atkins, P. W.; Kivelson, D. *J. Chem. Phys.* **1965**, *44*, 169.
(23) Edwards, J. T. *J. Chem. Educ.* **1970**, *47*, 261.
(24) Bordeaux, D.; Lajzerowicz-Bonneteau, J.; Brièr, R.; Lemaire, H.; Rassat, A. *Org. Magn. Reson.* **1973**, *5*, 47. Capiomont, A.; Chion, B.; Lajzerowicz-Bonneteau, J.; Lemaire, H. *J. Chem. Phys.* **1974**, *60*, 2530.
(25) Schaafsma, T. J.; Kivelson, D. *J. Phys. Chem.* **1968**, *49*, 1968.
(26) Su, G. *Ind. Eng. Chem.* **1946**, *38*, 803.
(27) Landolt-Börnstein. *Eigenschaften der Matrie in Ihren Aggregatzuständen IIa*; Schäfer, K., Lax, E., eds.; Springer-Verlag: Berlin, Göttingen, Heidelberg, 1960.